Variance and width of absorption lines of single molecules in low temperature glasses

Wolfgang Pfluegl, Frank L. H. Brown, and Robert J. Silbey

Citation: J. Chem. Phys. **108**, 6876 (1998); doi: 10.1063/1.476102
View online: http://dx.doi.org/10.1063/1.476102
View Table of Contents: http://jcp.aip.org/resource/1/JCPSA6/v108/i16
Published by the American Institute of Physics.

Variance and width of absorption lines of single molecules in low temperature glasses

Wolfgang Pfluegl, Frank L. H. Brown, and Robert J. Silbey
Department of Chemistry and Center for Materials Science and Engineering, Massachusetts Institute of Technology, Cambridge, Massachusetts 02139

(Received 17 October 1997; accepted 22 January 1998)

We consider the line shapes of single molecules in low temperature glasses due to dipole–dipole interaction between the molecules and other particles of the system. Motivated by computer simulations, we employ a simplified formula for the absorption lines and derive an analytic expression for the distribution of the variance of such absorption lines. The simplest version of this distribution—derived for pointlike particles without cutoff of the interaction at small distances—already accounts for the qualitative features of width histograms measured experimentally or gained by computer simulation. We further analyze the effect of the minimal approach distance between the chromophore and the perturbing particles and employ an approximate relation between the variance and the full width at half maximum of the absorption lines. We find that the main characteristics of the histogram of widths stem from the (homogeneous) distribution of interactions in space and do not reflect the distribution of the internal parameters of the underlying model. © *1998 American Institute of Physics.* [S0021-9606(98)51016-1]

I. INTRODUCTION

The line shape of an optical transition in a chromophore embedded in a glass at low temperatures depends sensitively on the environment of the chromophore. Dynamic fluctuations in the surrounding molecules cause the optical transition frequency to vary with time in a stochastic manner, giving rise to nonstandard line shapes. Thus a spectroscopic study of the line shapes of molecules embedded in glasses can, in principle, give information about the structure and dynamics of the surroundings of that molecule.[1–14]

A theoretical framework for analyzing the distribution of single molecule line shapes in low temperature glasses has been given by Geva and Skinner.[15–17] In their work, they derive the line shape of a chromophore in a glass at low temperature using the standard tunneling model[18–23] for the dynamics of the modes (called two-level systems or TLS) in the glass that affect the spectral transition. Using this formula, they employed Monte Carlo simulations to calculate the distribution of single molecule line shapes. In particular, they focused on the distribution of linewidths. The model had only one fitting parameter: the strength of the interaction between the two-level system dipole and the chromophore dipole (the distance dependence is taken to be r^{-3}). The results of their numerical work showed that the histogram representing the distribution of linewidths calculated from their model agreed with the histogram of experimental results, within the experimental error. This was a major step forward in that it showed that the standard tunneling model, which is well-studied theoretically, can account for the single molecule experimental results.

In the present paper, we employ the same model and show first that a simplification of the line shape formula can be made that does not significantly alter the results of the simulations of Geva and Skinner. Using this simplified formula allows us to derive an analytic form for the normalized distribution of linewidths that depends on two parameters: the interaction strength mentioned above and a cutoff radius in the interaction. The results are weakly dependent on the latter. The analytic form agrees quite well with the simulation results of Geva and Skinner[17] and also the experimental results.[24]

The paper is organized as follows: Sec. II states the model and the line shape formula, from which we calculate the first two moments and derive the variance distribution in Sec. III. Section IV compares these results with experiment and computer simulations, for which it is necessary to relate the variance to the width of the absorption lines and to consider the cutoff at small distances between the chromophore and the TLS. The final section contains some further remarks and our conclusions.

II. ABSORPTION LINES OF SINGLE MOLECULES IN THE SLOW MODULATION LIMIT

The absorption line of an individual chromophore coupling to n uncorrelated two-level systems (TLS) by dipolar interaction has been derived many times within the stochastic sudden-jump model.[15,16,25–28] In order to keep this article self-contained and to introduce the notation we briefly restate this theory: Every flip of a TLS is assumed to shift the transition frequency of the chromophore by an amount

$$\nu_j = \alpha \frac{\varepsilon_j}{r_j^3}, \tag{1}$$

where j labels the TLS, r_j is its distance from the chromophore, and ε_j is an orientation parameter, to be taken 1 or -1 with equal probability. α is the coupling constant for the TLS–chromophore interaction.[15,17,28,29] The dipole autocorrelation function for each of the TLS is given by[27,30]

$$\Phi_j(t)=\langle e^{-2\pi i\nu_j\int_0^t d\tau\xi_j(\tau)}\rangle. \tag{2}$$

The average is to be taken over all realizations of the stochastic variable $\xi_j(\tau)=0$ or 1, corresponding to the jth TLS being in the ground state or excited state at time τ, respectively, within the time interval $[0,t]$. The average of $\xi_j(\tau)$ is denoted by p_j, equal to the equilibrium occupation probability of the excited state of the jth TLS.

Formula (2) includes only the shift of the transition frequency relative to the electronic transition frequency when each of the TLS is in the ground state. All TLS which do not flip during the measurement would contribute to the frequency origin only, and not to the linewidth. The origin of the transition frequency is clearly not relevant for the variance of the absorption line, which we shall calculate in the next section. Therefore only those TLS that are not frozen during the measurement are taken into account for the line shape, i.e., n is related to the measuring time τ_m by

$$n(\tau_m)=\sum_i \theta(K_i-1/\tau_m), \tag{3}$$

with θ the Heaviside function and K_i the sum of the upward and downward flipping rate of the ith TLS.

Evaluating Eq. (2) one obtains[27,28,31,32]

$$\Phi_j(t)=e^{-\frac{1}{2}(K_j+2\pi i\nu_j)t}\left[\cosh\,\Omega_j t+\frac{\alpha_j}{\Omega_j}\sinh\,\Omega_j t\right], \tag{4}$$

where

$$\Omega_j=\sqrt{\frac{K_j^2}{4}-\pi^2\nu_j^2+2\pi i(\tfrac{1}{2}-p_j)\nu_j K_j} \tag{5}$$

and

$$\alpha_j=\frac{K_j}{2}+2\pi i(\tfrac{1}{2}-p_j)\nu_j. \tag{6}$$

For systems where we may neglect the natural lifetime T_1 of the excited state of the chromophore ($T_1\to\infty$), the absorption line is given by the Fourier transform of the total dipole autocorrelation function,

$$I_{SM}(\nu)=\int_{-\infty}^{\infty} dt\; e^{2\pi i\nu t}\prod_{j=1}^{n}\Phi_j(t). \tag{7}$$

Thus, the exact result given in Eqs. (4)–(6) may be used to obtain any desired property of the absorption line of the chromophore from Eq. (7). This treatment has been recently employed to calculate the full width at half maximum (FWHM) of absorption lines in computer simulations which chose the values for K_j, p_j, and r_j according to the standard tunneling model (STM).[15,17]

Here we restrict ourselves to systems for which the line broadening by the natural lifetime and by dephasing is small compared to the effect of spectral diffusion,

$$2\pi T_1,\pi T_2\gg\langle\Delta\nu\rangle^{-1}, \tag{8}$$

where T_2 is the time constant for dephasing and $\langle\Delta\nu\rangle$ the mean FWHM of the absorption lines obtained from different realizations of the system. For such a system, simulations[33] using the same procedure as described in Ref. 17, except that K_j was set to zero in Eqs. (4)–(6) for all the n active TLS, showed almost no difference with the full treatment. Figure 1 compares both models, using the (physical) parameters quoted and derived in Ref. 17 for the chromophore terrylene (Tr) embedded in polystyrene (PS). The distribution measured experimentally[24] is shown in the inset. All distributions of $\Delta\nu$ (the FWHM) are normalized. Compared to the discrepancy between computer simulations and experiment, the qualitative and also quantitative features of the two theoretical calculations are nearly identical.

By setting the flip rates, K_j, to zero we are neglecting all inherently dynamical effects such as motional narrowing. We include, however, the fact that each TLS may reside in one of two states with relative occupation probabilities dictated by the Boltzmann factors, p_j. In essence, we have reduced the full correlation function to that which would be obtained for an ensemble average of *static* environments around the chromophore, which might be justified for times large enough with regard to dephasing and motional narrowing and a distribution of K broad enough. In this sense, one might say that our expression for a single chromophore's homogeneous line is nothing more than the inhomogeneous line shape for a chromophore in interaction with point defects located at distances r_j with probability p_j. However, we should reiterate that the homogeneous broadening is replaced by the inhomogeneous only in as far as a subensemble of all TLS ($K_i>1/\tau_m$) is taken into account.

Based on these arguments, we use the following model in what follows: As in the STM, all TLS are distributed homogeneously in space. Thus the probability of finding a TLS at distance r is

$$p_r(r)=\frac{4\pi\rho}{n}\,\theta(r-r_c)\,\theta\left(\sqrt[3]{\frac{3n}{4\pi\rho}+r_c^3}-r\right)r^2. \tag{9}$$

Here ρ is the density of contributing TLS (n divided by the sample size). The cutoff r_c denotes the smallest distance between any TLS and the chromophore and shall be discussed later. The upper bound (the second Heaviside function) is simply determined by the number and the density of the TLS.

We do not assume any correlation between r_j and p_j, and replace p_j by an average excitation probability p.[34] For deriving the formulae of the next sections we do not have to make any specific assumptions concerning the distributions of the asymmetry A and the energy splitting E of the TLS, since we set all $K_j=0$. For completeness we remark that this step is consistent with putting $A_j/E_j=1$, a factor that was present on the right-hand side of Eq. (1) when using the STM. Last, we recall that T_1 and $T_2\to\infty$. Their contributions to the absorption lines may be taken into account as an overall effect applied to our final results, as long as the time scales are different.

For this model Eqs. (4)–(6) now reduce to

$$\Phi_j=1-p+pe^{-2\pi i\nu_j t}. \tag{10}$$

We see that the stochastic frequency trajectory of one TLS is reflected only by the average excitation probability p and its frequency shift ν_j.

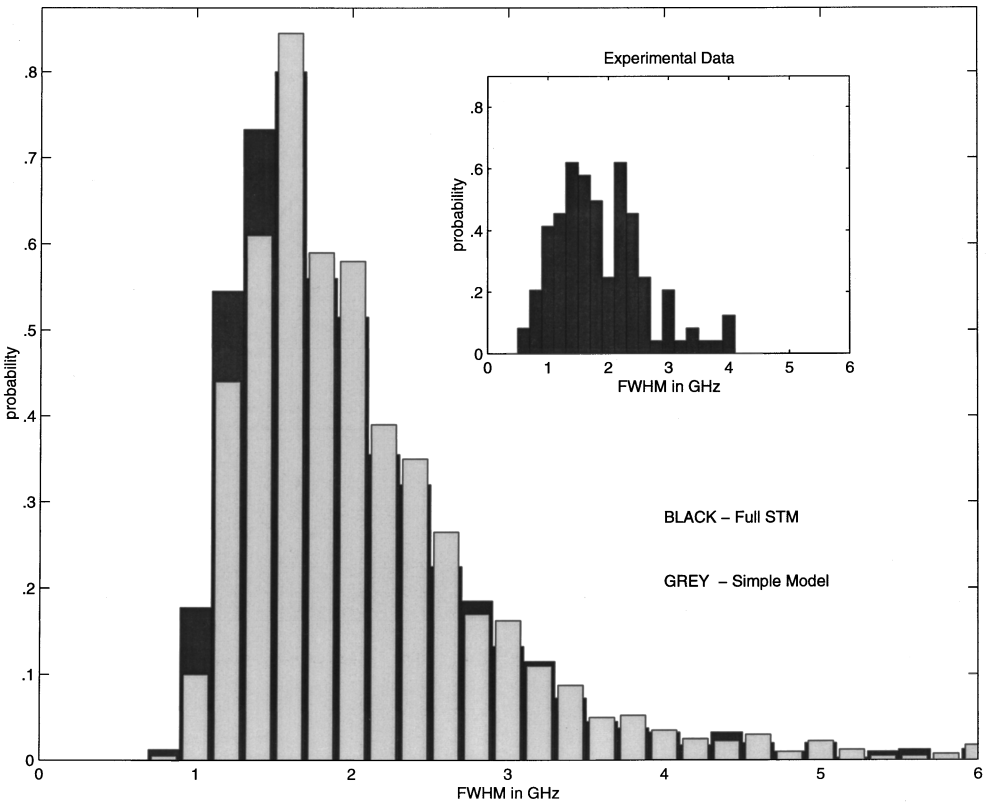

FIG. 1. Histogram of linewidths (FWHM): Comparison between the full treatment of the STM model (black) and our simple model with $K=0$ (grey). The inset shows the experimental data from Ref. 24.

III. THE DISTRIBUTION OF THE VARIANCE OF THE ABSORPTION LINES

From Eqs. (7) and (10) we derive the first two moments of the single molecule absorption line to be[35]

$$m_1^{(n)}=m_1^{(n-1)}+p\nu_n=p\sum_{j=1}^{n}\nu_j, \tag{11}$$

$$m_2^{(n)}=m_2^{(n-1)}+2p\nu_n m_1^{(n-1)}+p\nu_n^2; \quad m_2^{(1)}=p\nu_1^2, \tag{12}$$

where (n) refers to the number of TLS taken into account. We note that this is a result of our approximation $T_1\rightarrow\infty$, replacing the Lorentzian broadened lines by a set of differently weighted delta functions. The moments would diverge for a finite T_1.

The variance,

$$\sigma_{SM}^2=\int(\nu-m_1)^2 I_{SM}(\nu)d\nu, \tag{13}$$

turns out to be

$$\sigma_{SM}^2=\sum_{j=1}^{n}p(1-p)\nu_j^2. \tag{14}$$

Now we introduce dimensionless units,

$$\hat{\nu}=\nu\Big/\left(\frac{4\pi\rho}{3}\,\alpha\sqrt{p(1-p)}\right), \tag{15}$$

$$\hat{r}=r/r_0=r\sqrt[3]{\frac{4\pi\rho}{3}}, \tag{16}$$

where $4\pi r_0^3/3$ is the average volume in the sample with one TLS. Using Eqs. (1), (15), and (16) we obtain

$$\hat{\sigma}_{SM}^2=\sum_{j=1}^{n}\hat{r}_j^{-6} \tag{17}$$

for a single molecule and

$$g_n(\hat{\sigma}^2)=\int\delta\left(\sum_1^n\hat{r}_j^{-6}-\hat{\sigma}^2\right)\prod_j^n p_r(\hat{r}_j)d\hat{r}_j \tag{18}$$

for the distribution of the variance, when choosing different realizations of a system with n TLS according to our model, i.e., for different single molecules. The integrations are only over the radial positions of the TLS because σ^2 does not depend on ε_j (parallel or antiparallel dipole alignment). The only remaining internal parameter of the TLS, the excitation probability p, has been averaged already and does not appear in the formula because of the special choice of units.

The integrations are straightforward for a few TLS. For large n we use the Fourier representation of the delta function and obtain in the thermodynamic limit[36–38]

$$g_c(\hat{\sigma}^2)=\frac{1}{\pi}\int_0^\infty dx\; e^{\hat{r}_c^3(1-\cos x/\hat{r}_c^6)-2\sqrt{x}\int_0^{\sqrt{x}/\hat{r}_c^3}dz\,\sin z^2}\times\cos\left(\hat{\sigma}^2x+\hat{r}_c^3\,\sin\frac{x}{\hat{r}_c^6}-2\sqrt{x}\int_0^{\sqrt{x}/\hat{r}_c^3}dz\,\cos z^2\right). \tag{19}$$

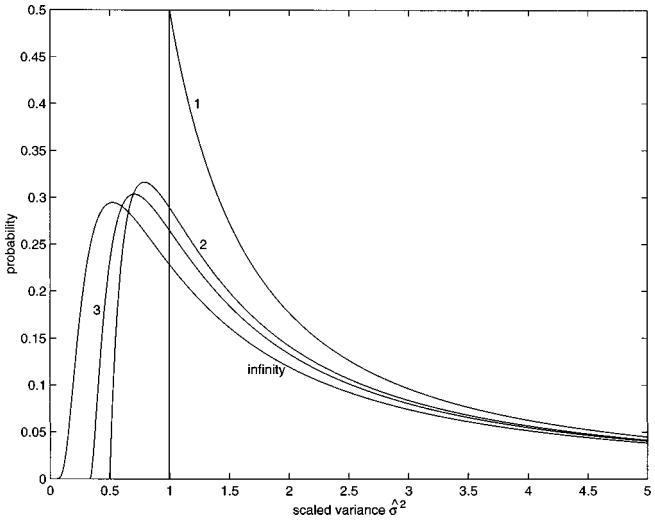

FIG. 2. Distribution of the scaled variance for systems with 1, 2, 3 and ∞ TLS, without cutoff ($\hat{r}_c=0$).

The subscript c denotes that the distribution depends on the cutoff $\hat{r}_c$. As a first approximation one might take the limit $\hat{r}_c \downarrow 0$, i.e., neglect the cutoff. In this case Eq. (19) simplifies to

$$g(\hat{\sigma}^2)=\frac{1}{2\hat{\sigma}^3}\exp\left(-\frac{\pi}{4\hat{\sigma}^2}\right). \tag{20}$$

Details of the derivation of Eqs. (19) and (20) as well as the formulae for the distributions g_1, g_2, and g_3 (systems with $n=1,2,3$ without cutoff) are given in Appendix A. These distributions and $g(\hat{\sigma}^2)$ (for $n\to\infty$) are shown in Fig. 2. Clearly, we expect the tail for large $\hat{\sigma}^2$ to be too large because of the unphysical contributions from neglecting the cutoff radius. Nevertheless, it is interesting to compare these distributions without cutoff. This is not only because of their rather simple form, which can still be derived analytically, but also for the fact of how nicely the series is able to demonstrate the gradual crossing from the well known distribution g_1[39] to that for $n=\infty$. Remembering the variety of SM line shapes[17,33] that can be created by the interaction with the TLS, it is surprising that an approximation using two or three TLS is able to capture the qualitative features of the variance distribution for large n. However, there are two reasons for this important finding: First, the distribution is an averaged quantity, where a lot of detailed information is already lost. Second, in many cases the skeleton of an absorption line is already given by the most dominant TLS, which are not necessarily the closest to the chromophore, but those with large $p_j(1-p_j)/r_j^6$.

IV. COMPARISON WITH EXPERIMENTS AND SIMULATIONS

In order to compare with the experiment and simulations we have to consider two particular aspects: The smallest distance between chromophore and TLS (r_c)[40] and the relation between variance and FWHM.

There is no way to avoid the cutoff r_c if we want to describe the physics correctly. Its relevance is illustrated immediately by calculating the average variance from Eqs. (9) and (17):

$$\langle\hat{\sigma}^2\rangle=\frac{1}{\hat{r}_c^3}\left(1-\frac{\hat{r}_c^3}{n+\hat{r}_c^3}\right). \tag{21}$$

Not surprisingly, this quantity diverges for $r_c\downarrow 0$.[42] Physically, a TLS cannot be infinitesimally close to the chromophore and r_c should be (at least) the size of a TLS and the chromophore, respectively. This is of the order of 1 nm, which corresponds to $\hat{r}_c\sim 0.4$ for Tr/PS with the TLS density ρ derived from Ref. 43.[44] But as Geva and Skinner pointed out,[17] the density values in the literature deviate by more than an order of magnitude for the same material.[43,45,46] Therefore, the uncertainty of $\hat{r}_c$ comes not only from the question of how close a TLS—acting still like a dipole—might be to the chromophore, but also from the value of ρ. Furthermore, we believe that the physical $\hat{r}_c$ mentioned above is only a lower bound for the results obtained in experiments and simulations, since it does not reflect either the procedure of measurement or that of the simulation. If a nearby flipping TLS splits the absorption line into two distinct peaks which are far away from each other (which would be the case for $\hat{r}_c$ very small), such a situation will be treated in experiments as two absorption lines of two different chromophores, and not as a single line.[47] In the simulations, these cases would be either discarded or kept, depending on the definition of the linewidth. In this manner, a nonphysical cutoff will be imposed. Consequently, we have to choose $\hat{r}_c$ to be the distance where line broadening becomes line splitting rather than the smallest possible physical distance. When the line is split into two equally high peaks, this corresponds to $\hat{r}_c^3\approx 0.4$. A detailed description is given in Appendix B. For different weighted peaks, the cutoff might be larger and is difficult to determine quantitatively. But even if we had a more precise number, this would refer to the procedures of measuring and defining the widths rather than to the underlying physical structures. Therefore we shall present the consequences of a finite cutoff by comparing the distributions for three different values of $\hat{r}_c^3$ ($\hat{r}_c^3=0.4,0.7,1.0$) in the following. Figure 3 shows how the shape of the distributions of the scaled standard deviation $\hat{\sigma}$ is altered, comparing the distributions with cutoff

$$h_c(\hat{\sigma})=2\hat{\sigma}g_c(\hat{\sigma}^2), \tag{22}$$

calculated numerically from Eq. (19), and the one without cutoff,

$$h(\hat{\sigma})=\hat{\sigma}^{-2}\exp\left(-\frac{\pi}{4\hat{\sigma}^2}\right). \tag{23}$$

The expected behavior is confirmed. The long tail of $h(\hat{\sigma})\sim 1/\hat{\sigma}^2$ is missing and consequently the maximum increases due to the normalization, the more the larger $\hat{r}_c^3$. The leading edge is not affected qualitatively. If $\hat{r}_c$ were the same for different systems, $h_c(\hat{\sigma})$ would represent a scaled master curve, independent of α, ρ, and other system parameters. The picture for $g_c(\hat{\sigma}^2)$ is completely analogous.

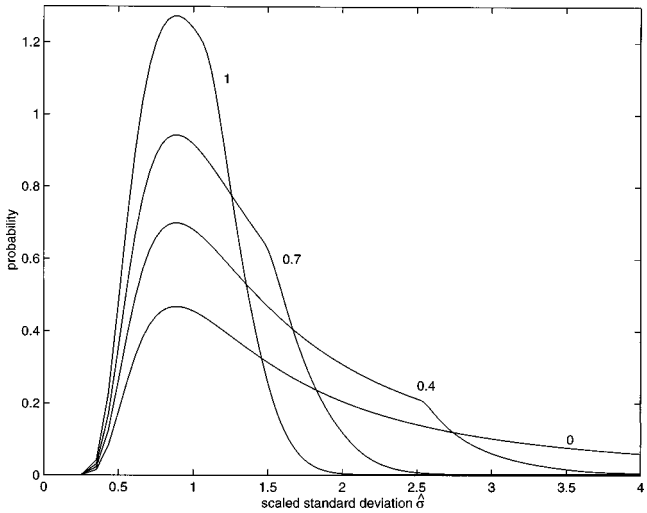

FIG. 3. Distribution of the standard deviation in dimensionless units for different cutoffs ($\hat{r}_c^3=1$, 0.7, 0.4, and 0).

The cutoff also influences the relation between σ and $\Delta\nu$. Since $\Delta\nu$ is used in the literature (see Fig. 1), we need such a relation in order to compare with the distributions g and h, respectively. In general, the ratio

$$q_{SM}=\Delta\nu_{SM}/\sigma_{SM} \tag{24}$$

is different for every single line, depending on its specific shape. However, as we use it for an averaged quantity, we assume it is reasonable to approximate all the q_{SM} by the ratio of the averages[49]

$$q=\langle\Delta\nu\rangle/\langle\sigma\rangle=\sqrt{\langle\Delta\nu^2\rangle/\langle\sigma^2\rangle}. \tag{25}$$

The second equality follows from the approximation of the different q_{SM} by a single factor, q, and the denominator is given by (21). Hence,

$$q=\sqrt{\langle\Delta\hat{\nu}^2\rangle}\hat{r}_c^{3/2}\sim(\hat{\gamma}/\pi)\hat{r}_c^{3/2}. \tag{26}$$

The FWHM of the average line shape, γ/π, can be calculated [see Eqs. (B1), and (A6) of Ref. 17] and has approximately the value of the root mean squared FWHM. According to our simulation, the latter is larger than γ/π by 17%, which is a small correction compared to the uncertainty of $\hat{r}_c$. With the parameters used in Fig. 1, q is approximately 0.5 and 0.7 for $\hat{r}_c^3$ equal to 0.4 and 1. Restoring the dimensions we finally obtain the scaling factor

$$\Delta\nu/\hat{\sigma}=1.17\,\frac{4\pi^2}{3}\,\rho\alpha\overline{p}\hat{r}_c^{3/2}\approx 2.2\ \text{GHz}\ \hat{r}_c^{3/2}, \tag{27}$$

where we have used the same parameters as in Fig. 1.[50] By means of this relation we may compare our analytically derived distributions with the simulations and the experimental histogram presented in Fig. 1. The plots are shown in Fig. 4. Again we have used the values $\hat{r}_c^3=0.4$, 0.7, and 1.0 for comparison. For illustration, the distribution without cutoff has also been included; it is scaled by 1.84 GHz, corresponding to $\hat{r}_c^3=0.7$. All plots are shifted by $\nu_s=0.17$ GHz to account for dephasing ($1/\pi T_2=0.13$ GHz) and lifetime broadening ($1/2\pi T_1=0.04$ GHz, both values from Ref. 17).

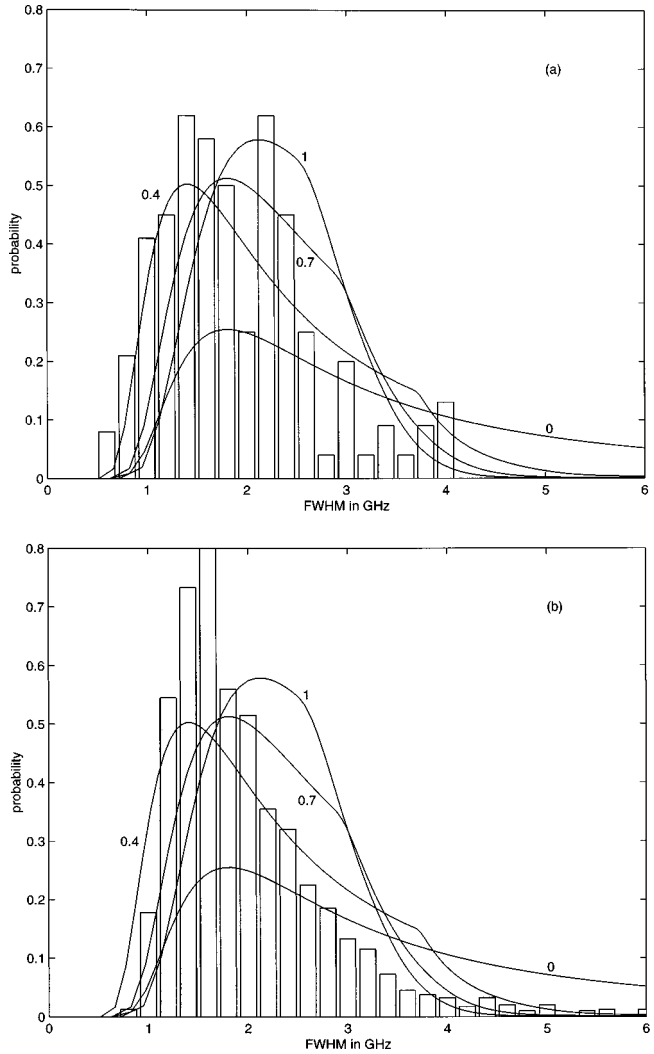

FIG. 4. Distribution of linewidths (FWHM): Calculation for different cutoffs ($\hat{r}_c^3=1$, 0.7, 0.4, and 0) compared to experiment (a) and simulation (b). The full STM model has been used for the simulation. The scaling factor for the plot without cutoff ($\hat{r}_c=0$) is 1.84 GHz (see text).

Because the cutoff also enters the scaling relation, the height and width of the distributions depend more weakly on $\hat{r}_c$ than in Fig. 3. The cutoff, however, still determines the skewness: for larger $\hat{r}_c$ the plots become more symmetric. So the main qualitative features of the histograms—a steeper wing on the left side compared to the longer tail on the right side—can be attributed to the distribution of TLS in space rather than to the distributions of their internal parameters.

V. CONCLUDING REMARKS

The most intriguing conclusion perhaps is that we may set $K_j=0$ for the systems under consideration and still recover the overall shape of the histograms measured and simulated, respectively. In hindsight, however, it turns out consistently that the most dominant TLS are those with the smallest K_j, but still within the range of the measuring time, because the TLS with the smallest distance and the largest excitation probability contribute most to σ_{SM} [Eqs. (1) and (14)], i.e., the frequency shift ν_j has to be large and the energy splitting E_j has to be small for dominant TLS (the

latter follows from $p_j = 1/(1+\exp E_j/kT)$ with k the Boltzmann constant and T the temperature). As small E_j implies small K_j, the relation $\nu_j \gg K_j$ used for the static approximation of Eq. (4) picks out the more dominant TLS. In addition to the simulation, an error estimate may be obtained by comparing the FWHM of the average line shape derived from the full treatment of the STM with the value of our simple model [Eq. (B1)]. For Tr/PS, this is 1.89 GHz (simple model) compared to 1.72 GHz (Table II of Ref. 17). Our value is expected to be higher because we have omitted the factor A_j/E_j in Eq. (1), which is always smaller than 1.

Moreover, we have demonstrated that systems with just a few TLS are sufficient to provide a good approximation to the thermodynamic limit of the histograms. We attribute this feature mainly to the fact that the histograms involve ensemble averaging. This indicates clearly that a lot of detailed information is lost in the histograms. Focusing on linewidth using the definitions usually employed cannot obtain all of the interesting structure of the line shapes and dynamics.

Although the qualitative features of the histogram can already be obtained from a distribution of the TLS in space without a cutoff boundary at the chromophore, such a cutoff is significant and physically necessary. It changes the shape of our distributions in the anticipated way and becomes important for the relation between σ and the FWHM of the line shapes. The latter consequence is not too surprising, because lines without cutoff, e.g., a Lorentzian, would entail divergent moments and thus become untractable.

Besides an estimate for $\hat{r}_c$, the relation between σ and the FWHM includes an approximation assuming the average homogeneous line shape to be typical. Thus, it would be preferable to compare the *distribution of* σ with experiments instead of that of the FWHM for more accurate quantitative conclusions.

In total we have four system parameters: α, ρ, p, and r_c. ρ is always linked either with α or with r_c^3. It is interesting that it is the scaled cutoff $\hat{r}_c$ rather than r_c which becomes important unless a nonphysical cutoff is imposed. If there were systems with very different ρ and comparable r_c, this should lead to a qualitative change of the distributions as shown in Figs. 3 and 4. However, only polymers with similar density have been investigated so far, and the uncertainty in the parameters involved does not allow for final conclusions. Also, the dependence of ρ on the measuring time should be reflected in a similar manner: ρ becomes larger and the distribution more symmetric for longer times. In principle, this determines an evolution in time of the distribution of widths.

The average excitation probability p and the effective density ρ depend on the temperature. We have used the full STM to calculate their values. Nevertheless, our results do not constitute a severe test of the STM as the dependence is too weak and essentially only contains the scaling parameter.

The main purpose of this work was to explain the distinct features of the histogram of widths and to investigate to what extent they reflect the specific assumptions of the STM. We have given simple relations between the width distribution and the underlying model for the case of small dephasing and lifetime broadening. It turned out that the main characteristics are due to the statistics arising from the random distribution of TLS in space. Thus such a histogram may not be very fruitful in investigating the dynamics, but may be used to determine the coupling constant between chromophore and TLS (multiplied by the effective density of TLS) and an estimate for the smallest distance between TLS and chromophore.

ACKNOWLEDGMENTS

We thank Peter Neu, David R. Reichman, and Jim Skinner for helpful discussions. The work has been supported in part by the National Science Foundation. F.L.H.B. thanks the National Science Foundation for a predoctoral fellowship. W.P. acknowledges financial support by the Austrian ''Fonds zur Förderung der wissenschaftlichen Forschung,'' Grant No. J01321-PHY.

APPENDIX A: DERIVATION OF THE FUNCTIONS G_1, G_2, G_3 AND EQS. (19) AND (20)

First we consider the case of $r_c = 0$. The formulae for g_1, g_2, and g_3 are obtained directly from Eq. (18) by inserting Eq. (9) with $n = 1,2,3$ and using Eq. (16). The result becomes lengthier and lengthier for higher n because of the boundaries of the integrals, which stem from the second Heaviside function in Eq. (9),

$$g_1(\hat{\sigma}^2) = \frac{1}{2\hat{\sigma}^3}\,\theta(\hat{\sigma}-1), \tag{A1}$$

$$g_2(\hat{\sigma}^2) = \frac{1}{4\hat{\sigma}^4}\left(\sqrt{4\hat{\sigma}^2-1} - \frac{1}{\sqrt{4\hat{\sigma}^2-1}}\right)\theta\left(\hat{\sigma}-\frac{1}{\sqrt{2}}\right), \tag{A2}$$

$$g_3(\hat{\sigma}^2) = \frac{1}{2\hat{\sigma}^3}\left\{\frac{(3\hat{\sigma}^2-1)\sqrt{9\hat{\sigma}^2-2}}{\hat{\sigma}(9\hat{\sigma}^2-1)} + \frac{1}{9\hat{\sigma}^2}\left[\arctan\frac{6\hat{\sigma}\sqrt{9\hat{\sigma}^2-2}}{(9\hat{\sigma}^2-1)^2-2} - \arctan(3\hat{\sigma}\sqrt{9\hat{\sigma}^2-2})\right]\right\}\theta\left(\hat{\sigma}-\frac{1}{\sqrt{3}}\right). \tag{A3}$$

For large n we have

$$g(\hat{\sigma}^2) = \frac{1}{2\pi}\int_{-\infty}^{\infty} dx\; e^{-ix\hat{\sigma}^2}\exp\left[\int_0^{\infty}(e^{ix\hat{r}^{-6}}-1)\,d\hat{r}^3\right], \tag{A4}$$

where we have used the Fourier representation of the delta function in Eq. (18) and taken the thermodynamic limit. The inner integral is evaluated by partial integration after substitution, which leads to Fresnel integrals of value $(1/2)\sqrt{\pi/2}$,

$$\int_0^{\infty}(1-e^{ixr^{-6}})\,dr^3 = \sqrt{|x|}\,\sqrt{\frac{\pi}{2}}\,(1-i\ \mathrm{sign}\ x). \tag{A5}$$

Hence,

$$g(\hat{\sigma}^2) = \frac{1}{\pi}\int_0^{\infty} dx\; e^{-\sqrt{\pi x/2}}\cos\left(\hat{\sigma}^2 x - \sqrt{\frac{\pi x}{2}}\right). \tag{A6}$$

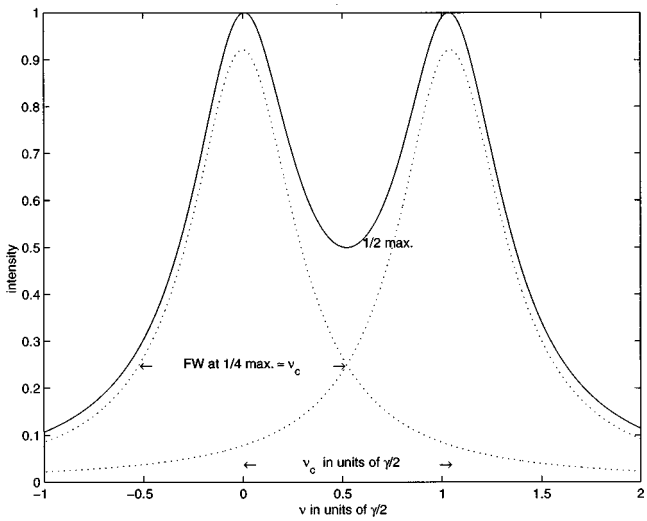

FIG. 5. Approximate line shape caused by a close TLS with $p_1=1/2$.

Using $\cos(a-b)=\cos a\cos b+\sin a\sin b$, g turns out to be the sum of the Fourier cosine transform of $(1/\pi)\times\exp(-\sqrt{\pi x/2})\cos\sqrt{\pi x/2}$ and the (identical) Fourier sine transform of $(1/\pi)\exp(-\sqrt{\pi x/2})\sin\sqrt{\pi x/2}$, presented in Eq. (20). For finite r_c, expression (A5) has to be replaced by

$$\int_{\hat r_c^3}^{\infty}(1-e^{ixr^{-6}})dr^3$$

$$=2\sqrt{|x|}\left(\int_0^{\sqrt{x}/\hat r_c^3}dz\ \sin z^2-i\ \mathrm{sign}\ x\int_0^{\sqrt{x}/\hat r_c^3}dz\ \cos z^2\right)$$

$$-\hat r_c^3\left(1-\cos\frac{x}{\hat r_c^6}-i\ \sin\frac{x}{\hat r_c^6}\right), \tag{A7}$$

leading to Eq. (19). The further evaluation in this case was done numerically.

APPENDIX B: A CUTOFF TAKING INTO ACCOUNT THE REJECTION OF SPLIT ABSORPTION LINES

We consider the following situation (Fig. 5): The closest TLS at distance $\hat r_c$ gives rise to a frequency shift $\nu_c=\alpha/r_c^3$. The contributions of all the other TLS are small compared to ν_c. This assumption holds as long as r_c is small enough so that the probability for a second TLS to be about as close as r_c is vanishing. Taking average values for these TLS, they cause a Lorentzian broadening of each of the two frequencies spaced by ν_c. These Lorentzians correspond to the average SM line shape for large n, characterized by the FWHM,

$$\gamma/\pi=\frac{4\pi^2}{3}\alpha\rho\overline{p} \tag{B1}$$

(cf. A6 of Ref. 17).[50] For simplicity we have assumed equal height of the Lorentzians in Fig. 5 ($p_1=1/2$). If the minimum of this line shape lies above half the value of the maxima, the FWHM$\approx\nu_c+\gamma/\pi$ is unambiguously defined. If the minimum is below, however, different procedures for looking for the half maximum (e.g., starting from both sides of the frequency range and moving inward, or starting from a peak frequency and moving outward) will render different results. Discarding such lines (as is done in the simulations) means setting a cutoff at $\nu_c\approx$FW at a quarter of the maximum of one Lorentzian. From this condition we conclude

$$\nu_c=\sqrt{3}\gamma/\pi, \tag{B2}$$

and, using (16) and (B1),

$$\hat r_c^3=\frac{1}{\pi\sqrt{3}\overline{p}}\sim 0.37. \tag{B3}$$

[1] J. L. Skinner and W. E. Moerner, J. Phys. Chem. **100**, 13,251 (1996).
[2] R. M. Macfarlane and R. M. Shelby, J. Lumin. **7**, 179 (1987).
[3] D. Haarer and R. Silbey, Phys. Today **44**, 58 (1990).
[4] Proceedings of the Fifth International Meeting on Hole Burning and Related Spectroscopies (HBRS'96) Science and Applications (Brainerd, Minnesota, 1996), Vol. 291 of Mol. Cryst. Liq. Cryst., G. Small, editor.
[5] W. E. Moerner and L. Kador, Phys. Rev. Lett. **62**, 2535 (1989).
[6] M. Orrit and J. Bernard, Phys. Rev. Lett. **65**, 2716 (1990).
[7] W. E. Moerner and T. Basché, Angew. Chem. **32**, 457 (1993).
[8] M. Orrit, J. Bernard, and R. I. Personov, J. Phys. Chem. **97**, 10,256 (1993).
[9] U. P. Wild, M. Croci, F. Güttler, M. Pirotta, and A. Renn, J. Lumin. **60, 61**, 1003 (1994).
[10] T. Basché and C. Bräuchle, Ber. Bunsenges. Phys. Chem. **100**, 1269 (1996).
[11] W. E. Moerner, J. Lumin. **60**, 997 (1994).
[12] L. Kador, Phys. Status Solidi B **189**, 11 (1995).
[13] R. A. Keller, W. P. Ambrose, P. M. Goodwin, J. H. Jett, J. C. Martin, and M. Wu, Appl. Spectrosc. **50**, 12A (1996).
[14] T. Basché, W. Moerner, M. Orrit, and U. P. Wild, *Single-Molecule Optical Detection, Imaging, and Spectroscopy* (VCH, Weinheim, 1996).
[15] E. Geva, P. D. Reilly, and J. L. Skinner, Acc. Chem. Res. **29**, 579 (1996).
[16] E. Geva and J. L. Skinner, J. Chem. Phys. **107**, 7630 (1997).
[17] E. Geva and J. L. Skinner, J. Phys. Chem. B **101**, 8920 (1997).
[18] P. W. Anderson, B. I. Halperin, and C. M. Varma, Philos. Mag. **25**, 1 (1971).
[19] W. A. Phillips, J. Low Temp. Phys. **7**, 351 (1972).
[20] J. L. Black and B. I. Halperin, Phys. Rev. B **16**, 2879 (1977).
[21] R. Silbey, J. M. A. Koedijk, and S. Völker, J. Chem. Phys. **105**, 901 (1996).
[22] A. Heuer and R. Silbey, Phys. Rev. Lett. **70**, 3911 (1993).
[23] J. L. Skinner and H. P. Trommsdorf, J. Chem. Phys. **89**, 897 (1988).
[24] B. Kozankiewicz, J. Bernard, and M. Orrit, J. Chem. Phys. **101**, 9377 (1994).
[25] J. R. Klauder and P. W. Anderson, Phys. Rev. **125**, 912 (1962).
[26] A. Suárez and R. Silbey, Chem. Phys. Lett. **218**, 445 (1994).
[27] P. D. Reilly and J. L. Skinner, J. Chem. Phys. **101**, 959 (1994).
[28] J. L. Skinner, in *Single-Molecule Optical Detection, Imaging, and Spectroscopy*, edited by T. Basché, W. Moerner, M. Orrit, and U. P. Wild (VCH, Weinheim, 1996), p. 143.
[29] P. D. Reilly and J. L. Skinner, J. Chem. Phys. **102**, 1540 (1995).
[30] R. Kubo, Adv. Chem. Phys. **15**, 101 (1969).
[31] P. W. Anderson, J. Phys. Soc. Jpn. **9**, 316 (1954).
[32] R. Kubo, J. Phys. Soc. Jpn. **6**, 935 (1954).
[33] F. L. H. Brown, Ph.D. thesis, Massachusetts Institute of Technology, 1998.
[34] This average has to be defined by
$$\sqrt{p(1-p)}\coloneqq\int_0^{1/2}\sqrt{p'(1-p')}p_p(p')dp',$$
with $p_p(p')$ the probability that p_j has the value p' (for any j). Then Eq. (20) gives the exact result for any excitation probability distribution p_p, as can be seen from keeping the p_j's in Eqs. (A4) and (A5) and performing the average over $p_p(p_j)$.
[35] A. M. Stoneham, Rev. Mod. Phys. **41**, 82 (1969).
[36] A similar equation has been derived by Fleury (Ref. 37), (II-81), for the high temperature limit ($p=1/2$). Quite differently from our approach, he assumed the homogeneous linewidth to be large compared to the fre-

quency shifts ν_j. We thank J. Skinner for pointing out and sending us a copy of the Fleury Ph.D. thesis.
[37] L. Fleury, Ph.D. thesis, Université Bordeaux I, 1995.
[38] L. Fleury, A. Zumbusch, M. Orrit, R. Brown, and J. Bernard, J. Lumin. **56**, 15 (1993).
[39] G. Zumofen and J. Klafter, Chem. Phys. Lett. **219**, 303 (1994).
[40] The dependence of the distribution of width on the minimal approach distance between chromophore and TLS has also been addressed in Refs. 38 and 41.
[41] R. Brown and M. Orrit, in *Single-Molecule Optical Detection, Imaging, and Spectroscopy*, edited by T. Basché, W. Moerner, M. Orrit, and U. P. Wild (VCH, Weinheim, 1996), p. 109.
[42] $p_c(\hat{r})=3\hat{r}^2e^{-\hat{r}^3}$ gives the probability that the closest particle of a three-dimensional, homogeneous distribution is at a distance $\hat{r}$. As the frequency shift is proportional to the inverse cube of the distance, the weighted contribution of the closest TLS$\sim 1/\hat{r}$ diverges for $\hat{r}\downarrow 0$. The divergence holds for three dimensions or less.
[43] R. O. Pohl, in *Amorphous Solids, Low Temperature Properties*, edited by W. Phillips (Springer Verlag, Berlin, 1981), p. 27.
[44] For the specific system under consideration, the density of active TLS, which are not frozen during the measurement, is about 10% less than the density value used in Ref. 17. The density of active TLS may not be confused with the average density of thermally populated TLS, which is about an order of magnitude smaller for the specific case.
[45] J. F. Berret and M. Meissner, Z. Phys. B **70**, 65 (1988).
[46] K. A. Topp and D. G. Cahill, Z. Phys. B **101**, 235 (1996).
[47] Examples for line splitting can be found in Refs. 38 and 48. These experiments were done with the same chromophore (Tr), but embedded in different hosts (polyethylene and *n*-alkanes, respectively). In the latter, jumping lines were purposely excluded from the distributions of linewidths.
[48] M. Vacha, Y. Liu, H. Nakatsuka, and T. Tani, J. Chem. Phys. **106**, 8324 (1997).
[49] For a test of the quality of this approximation, it would be useful to have the distribution of the variance from the experimental data as well.
[50] The mean equilibrium excitation probability of the excited state $\overline{p}=\int_0^{1/2}p' p_p(p')\mathrm{d}p'$ differs (slightly) from p defined in Ref. 34.